THE JOURNAL OF PHYSICAL CHEMISTRY B

ARTICLE

pubs.acs.org/JPCB

Effect of Cholesterol on Binding of Amphipathic Helices to Lipid Emulsions

Mai Ozawa,[†] Tetsurou Handa,[‡] and Minoru Nakano*

Graduate School of Pharmaceutical Sciences, Kyoto University, Sakyo-ku, Kyoto 606-8501, Japan

ABSTRACT: Plasma triglyceride-rich lipoproteins vary in their lipid composition during metabolism. We investigated the effects of cholesterol (Chol) on the surface properties of lipid emulsions and on the interactions with two amphipathic peptides, acetyl-DWLKAFYDKVAEKLKEAF-amide (Ac-18A-NH_2) and acetyl-KWLDAFYDEVAEKLKKAF-amide (Ac-18G*-NH_2), which differ in charge distribution. The fluorescence lifetimes of *N*-dansyl phosphatidylethanolamine (dansyl-PE) and *n*-(9-anthroyloxy)stearic acid (*n*-AS, *n* = 2, 6, and 12) were used to assess the water penetration into the headgroup and acyl chain regions of phosphatidylcholine (PC), respectively. Steady-state fluorescence anisotropy of *n*-AS was also performed to evaluate the acyl chain fluidity in emulsion surface monolayers. Chol decreased the fluorescence lifetime of dansyl-PE and increased the lifetimes and anisotropy values of *n*-AS. These results demonstrated that Chol alters the surface properties of emulsions, i.e., induces PC headgroup separation and acyl chain condensation. The two peptides showed different responses to Chol in several experiments: Addition of Chol to emulsions decreased and increased the dissociation constants of Ac-18A-NH_2 and Ac-18G*-NH_2, respectively. Furthermore, the α-helical content of Ac-18A-NH_2 was decreased by Chol, whereas that of Ac-18G*-NH_2 was unchanged. The higher reduction in helicity for Ac-18A-NH_2 is probably due to its deeper penetration than Ac-18G*-NH_2 into the hydrocarbon region of surface monolayers in the absence of Chol, which was demonstrated by Trp quenching experiments with *n*-AS. From these results, the charge distribution of the amphipathic helices is suggested to be a determining factor in their response to Chol enrichment in emulsions.

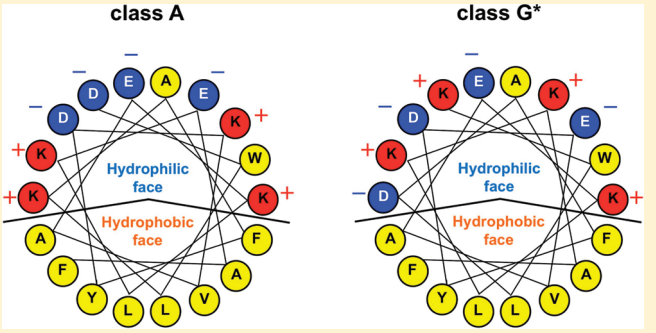

INTRODUCTION

Lipid emulsions composed of triglyceride (TG) cores and surface monolayers of phosphatidylcholine (PC) are protein-free models for TG-rich lipoproteins, such as chylomicrons and very low-density lipoproteins. In plasma, TG-rich lipoproteins vary in their lipid composition during metabolism, which alters surface properties[1−3] and distribution of exchangeable apolipoproteins and, accordingly, determines the fates of the particles themselves.[4−7] Particularly, the surface content of cholesterol (Chol) is thought to be an important factor regulating binding behavior of apolipoproteins.[8] In fact, several studies have shown that surface Chol affects the binding of apolipoproteins to lipid emulsions.[7−10]

Amphipathic α-helices, which are responsible for lipid binding of apolipoproteins, have been classified into several distinct classes according to the distribution of charged residues around the helix axis.[11,12] The class A helix is a major lipid-binding motif of exchangeable apolipoproteins and is characterized by the location of basic residues near the hydrophilic/hydrophobic interface and acidic residues clustered at the center of the polar face.[13] Class G* helix, which is distinguished by a random radial arrangement of positive and negative amino acid residues on the polar face, has also been identified in the exchangeable apolipoproteins. This type of amphipathic α-helix is proposed to have reduced lipid affinity.[13]

To explain the higher lipid affinity of the class A amphipathic helices, the "snorkel model" has been proposed.[11,14] According to this model, the interfacial location of the lysine residues in class A helices is suited for membrane interaction because of a strong hydrophobic interaction through their long hydrocarbon side chains and of a favorable electrostatic interaction through the positively charged ends with the phospholipid headgroup. This "snorkeling" allows greater penetration of class A amphipathic helices into the hydrophobic interior of phospholipid membranes.

Such structural elements have been suggested to play a crucial role in the formation of apolipoprotein−lipid complexes. In order to gain insight into the molecular mechanisms of the process, many studies have been attempted using model systems containing lipid vesicles, which are commonly used as models for biomembranes, and class A peptides.[15−19] One of the greatest concerns is the effect of Chol on the lipid-associating properties of class A peptides. Egashira et al. reported that addition of Chol to phospholipid vesicles increases the maximum binding amount and reduces the affinity of a class A peptide, accompanied by a change in its location in bilayers.[20] However, the binding properties of class A peptides in emulsions have not been studied in detail.

It is possible that the charge distribution of the amphipathic helices regulates their response to Chol in lipid emulsions, which

Received: July 24, 2011
Revised: November 17, 2011
Published: December 13, 2011

 © 2011 American Chemical Society dx.doi.org/10.1021/jp207062h | *J. Phys. Chem. B* 2012, 116, 476–482

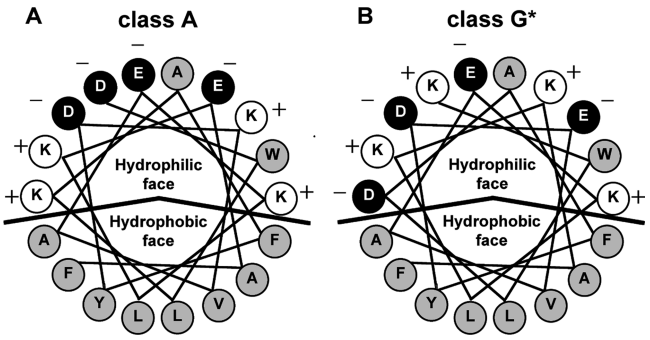

Figure 1. Helical wheel representations of class A amphipathic helix, Ac-18A-NH_2 (A), and class G* amphipathic helix, Ac-18G*-NH_2 (B). Symbols for positively charged, negatively charged, and hydrophobic residues are represented by white, black, and gray circles, respectively.

may lead to the exchange of apolipoproteins among plasma lipoproteins. The present study was undertaken to elucidate the influence of Chol in emulsions on the interaction with class A and G* model peptides on binding behavior, secondary structure, and location of the peptides. In addition to the well-studied class A model peptide, acetyl-DWLKAFYDKVAEKLKEAF-amide (Ac-18A-NH_2),[21,22] we designed and used the class G* peptide, acetyl-KWLDAFYDEVAEKLKKAF-amide (Ac-18G*-NH_2). These peptides have the same amino acid compositions but different charge distributions on the polar face (Figure 1). Because of the lysine substitution for negatively charged aspartic acid at the polar/nonpolar interface, a decreased "snorkel effect" is expected on the lipid binding of Ac-18G*-NH_2. The physical states of lipid emulsions were also evaluated in detail, using triolein-phosphatidylcholine (TO-PC) or triolein-phosphatidylcholine/cholesterol (TO-PC/Chol) emulsions, to explore the relationship between the binding behaviors of the helices and the membrane properties of emulsions.

EXPERIMENTAL SECTION

Materials. TO, Chol, and egg yolk phosphatidylcholine (PC) were purchased from Sigma Chemical Co. (St. Loui, MO). *N*-(5-Dimethylaminonaphthalene-1-sulfonyl) dipalmitoylphosphatidylethanolamine (dansyl-PE) was obtained from Avanti Polar Lipids (Alabaster, AL). A series of *n*-(9-anthroyloxy)stearic acids (*n*-AS, n = 2, 6, and 12) were from Invitrogen (Eugene, OR, for 2-AS and 12-AS) and Wako Pure Chemicals (Osaka, Japan, for 6-AS). Ac-18A-NH_2 and Ac-18G*-NH_2 (purity >95%) were purchased from Hayashi Kasei (Osaka, Japan). These products were used without further purification. All other chemicals were of the highest reagent grade.

Preparation of Emulsions. Two types of emulsions, Chol-free (TO-PC) emulsion and Chol-containing (TO-PC/Chol, with a molar ratio of PC/Chol =3:2) emulsion with diameters of 100−120 nm (determined from dynamic light scattering using FPAR-1000, Otsuka Electronic Co., Osaka, Japan), were prepared using a high-pressure emulsifier (Nanomizer System YSNM-2000AR; Yoshida Kikai Co., Nagoya, Japan) as described previously.[3,10,23] Briefly, a mixture of TO, PC, and Chol was suspended in 10 mM Tris-HCl buffer (pH 7.4) containing 150 mM NaCl, 1 mM EDTA, and 0.01% NaN_3 and successively emulsified under a pressure of 100 MPa. The vesicles contained were removed by ultracentrifugation (20 000 rpm for 1 h) with Beckman SW28 rotor (Fullerton, CA). The concentrations of PC, TO, and Chol were determined using enzymatic assay kits purchased from Wako Pure Chemicals (Osaka, Japan). The molar ratios of core TO to total surface PC for isolated TO-PC and TO-PC/Chol emulsions were 4.83 ± 0.21 and 4.72 ± 0.16, respectively (mean ± S.D., n = 8). The molar ratios of surface PC/Chol for isolated TO-PC/Chol emulsions were almost consistent with those of the starting mixtures (PC/Chol = 3:2).

Peptide-Binding Studies. Mixtures (500 μL) of a constant amount of emulsions (1 mM for TO) and various amounts of peptides were incubated for 1 h to equilibrate the free and bound peptides at 25 °C. Each mixture was ultracentrifuged (24 000 rpm for 1 h) with Beckman SW50.1 rotor to separate the bound (the top fraction) from free peptide (the bottom fraction, 200 μL). A centrifugation period of 1 h was selected to give stationary values of bound peptide. The bottom fractions were collected, and then 100 μL of 10% nonionic surfactant, heptaethylene glycol monododecyl ether, was added. The peptide concentration in the fraction was determined by measuring the peak area of Trp fluorescence near 335 nm (excitation at 280 nm). Free peptide in the same surfactant solution was used as a fluorescence standard. The amount of the lipid-bound peptide was calculated from the difference between the peptide concentrations before and after ultracentrifugation.[10,24] Binding data were analyzed according to the following equation[20]

$$\frac{P_b}{[TO]} = N\frac{P_f}{(K_d + P_f)} \quad (1)$$

where P_b and P_f are bound and free peptide concentrations (μM), respectively, [TO] is the concentration of TO in emulsions (mM), N is the binding maximum (mmol peptide/mol TO), and K_d is the dissociation constant (μM).

Fluorescence Measurements. For the fluorescence measurements, emulsions were prepared with a fluorophore to yield probe:PC ratios of 1:100 for dansyl-PE and 1:200 for *n*-AS. The fluorescence lifetime of dansyl-PE and *n*-AS were measured on a Horiba NAES-550 nanosecond fluorometer (Kyoto, Japan) with a pulsed hydrogen lamp (full width at half-maximum: ∼2 ns) at 25 °C. The samples labeled with dansyl-PE were excited through a Hoya U350 band-pass filter, and emission was observed through a Hoya Y48 cutoff filter. For *n*-AS, samples were excited through Hoya U360 (Tokyo, Japan) and Toshiba UV-34 filters (Tokyo, Japan) and detected through a $CuSO_4$ solution (250 g/L) and a Hoya L42 filter. The fluorescence decay curves were fitted as double-exponentials, with convolution of the intensity profile for pulsed excitation light by a Horiba NAES-5X0 lifetime analysis program. Total fluorescence decay $I(t)$ is expressed by the summation of exponential decay functions with the preexponential factor α_i and the fluorescence lifetime τ_i for the ith component:

$$I(t) = \alpha_1 \exp(-t/\tau_1) + \alpha_2 \exp(-t/\tau_2) \quad (2)$$

The mean fluorescence lifetime $\langle\tau\rangle$ was defined as

$$\langle\tau\rangle = \frac{\alpha_1\tau_1^2 + \alpha_2\tau_2^2}{\alpha_1\tau_1 + \alpha_2\tau_2} \quad (3)$$

Fluorescence emission spectra and steady-state fluorescence anisotropy measurements of *n*-AS and quenching experiments were performed with a Hitachi F-4500 spectrofluorometer at 25 °C using a 5 mm path-length cuvette. For the emission spectra and anisotropy measurements, the samples were excited at 385 nm. In the case of anisotropy measurements, the emission

was detected at 460 nm. The measured intensities were corrected by subtracting the blank sample containing an identical concentration of nonlabeled emulsion. The fluorescence anisotropy, r_s, is expressed by the equation

$$r_s = \frac{I_{VV} - GI_{VH}}{I_{VV} + 2GI_{VH}} \quad (4)$$

where I_{VH} and I_{VH} are the intensities of vertically and horizontally polarized fluorescent light, respectively, when excitation light is vertically polarized. The correction factor G, which is the ratio of the sensitivities of the detection system for vertically and horizontally polarized light, is represented as

$$G = I_{HV}/I_{HH} \quad (5)$$

where I_{HV} and I_{HH} are the intensities of vertically and horizontally polarized light, respectively, when excitation light is horizontally polarized.

The depth of penetration of the single peptide Trp residue inside the emulsion surface monolayers was measured by fluorescence quenching experiments. We used *n*-AS as Trp quenchers by fluorescence resonance energy transfer (FRET). Aliquots of peptide solution were added to *n*-AS-labeled (*n*-AS:PC ratio of 1:100) or nonlabeled emulsion suspensions to achieve conditions where the free fraction of peptide did not exceed 6% and incubated for 30 min before recording Trp fluorescence intensity (excitation at 285 nm and emission at 335 nm). When the peptide's Trp and anthroyloxy moieties of *n*-AS were in close proximity to each other, FRET from Trp to *n*-AS resulted in the reduction of Trp fluorescence. The intensity of an identical sample without peptide was also measured and subtracted from the observed value to reveal the quenching by *n*-AS. The extent of quenching was expressed as the value of F_0/F, where F_0 and F are Trp fluorescence intensities in the absence and presence of quencher, respectively.

CD Spectral Measurements. CD measurements were carried out to estimate the secondary structures of the peptides in a buffer, emulsions, and 50% (v/v) 2,2,2-trifluoroethanol (TFE) in a buffer. CD spectra were recorded from 195 to 250 nm with a JASCO J-720 spectropolarimeter at 25 °C. A 0.1 cm path-length cell was used to obtain the peptide spectra at 10 μM. The TO concentrations of emulsions were set to 390 and 720 μM for Ac-18A-NH_2 and Ac-18G*-NH_2, respectively, where about 40% of the peptides bind to emulsions. Eight (in TFE) or twenty (in buffer or emulsions) scans were recorded, averaged, and smoothed for each sample to improve the signal-to-noise ratio. The results were corrected by subtracting the buffer baseline or a blank sample containing an identical concentration of lipid or TFE. The α-helical contents were estimated from the following equation[25]

$$\%\alpha\text{-helix} = \frac{-[\theta_{222}] + 3000}{36000 + 3000} \times 100 \quad (6)$$

where $[\theta_{222}]$ is the mean molar residue ellipticity at 222 nm.

RESULTS

Effects of Chol on Surface Properties of Emulsions. To investigate the surface properties of the TO-PC and TO-PC/Chol emulsions, the fluorescence lifetimes of dansyl-PE and *n*-AS in emulsions were employed. Dansyl fluorophores are located in the PC headgroup region,[26,27] and the fluorophores of *n*-AS are in the hydrocarbon region of the membranes, depending on the position number *n*.[26,28] The fluorescence lifetime of these fluorophores is sensitive to the local polarity, to which the major contribution comes from water.[29,30] Therefore, these probes can detect the differences in lipid-packing states.[31−34] The fluorescence emission spectra of *n*-AS were also recorded to monitor changes in the local environment. As shown in Figure 2A, the mean fluorescence lifetime ($\langle\tau\rangle$) of dansyl-PE in emulsions significantly decreased in the presence of Chol, suggesting an increased water penetration into the headgroup region. In contrast, the lifetime of *n*-AS increased in the presence of Chol. Figure 2B

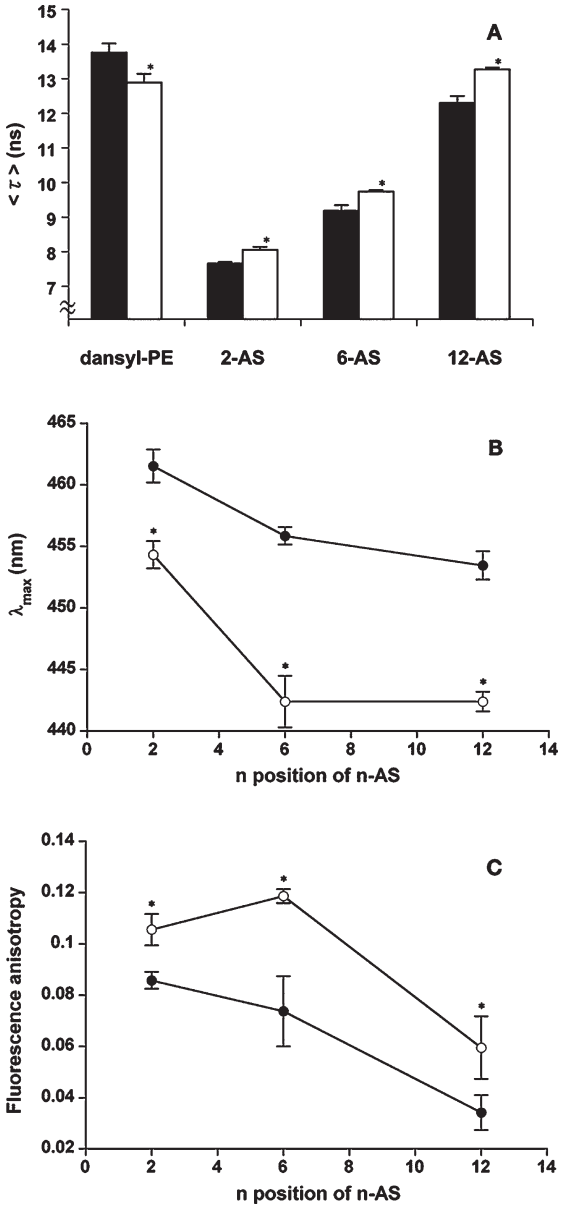

Figure 2. (A) Mean fluorescence lifetimes of dansyl-PE and *n*-AS in TO-PC (closed bars) and TO-PC/Chol (open bars) emulsions. *$p < 0.05$, significantly different from TO-PC emulsions. (B) Emission maximum wavelength (λ_{max}) of *n*-AS in TO-PC (closed circles) and TO-PC/Chol (open circles) emulsions. The λ_{max} values are plotted against *n*. *$p < 0.05$, significantly different from TO-PC emulsions. (C) Steady-state fluorescence anisotropy of *n*-AS in TO-PC (closed circles) and TO-PC/Chol (open circles) emulsions. The values are plotted against *n*. *$p < 0.05$, significantly different from TO-PC emulsions.

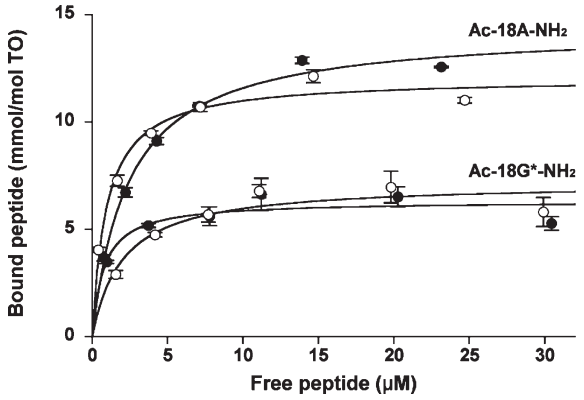

Figure 3. Binding profiles of Ac-18A-NH_2 and Ac-18G*-NH_2 in TO-PC (closed circles) and TO-PC/Chol (open circles) emulsions at 25 °C. The lines are theoretical curves calculated using the K_d and N values listed in Table 1.

Table 1. Binding parameters of Ac-18A-NH_2 and Ac-18G*-NH_2 to TO-PC and TO-PC/Chol Emulsions[a]

	Ac-18A-NH_2		Ac-18G*-NH_2	
	K_d (μM)	N (mmol/mol TO)	K_d (μM)	N (mmol/mol TO)
TO-PC	2.41 ± 0.27	14.4 ± 0.4	0.76 ± 0.33	6.31 ± 0.39
TO-PC/Chol	0.96 ± 0.18	12.0 ± 0.4	2.02 ± 0.76	7.18 ± 0.57

[a] Errors for K_d and N values were estimated from regression analysis.

shows the emission maximum of *n*-AS, which represented a blue shift by the incorporation of Chol for each *n*. These results indicate a decreased polarity (water accessibility) in the acyl chain region. We also measured the steady-state fluorescence anisotropy of *n*-AS (Figure 2C), which reports on the acyl chain packing and lipid order in emulsion surface monolayers. The anisotropy values of *n*-AS in TO-PC/Chol emulsions were much higher than those in TO-PC emulsions, suggesting that Chol causes condensation of the acyl chain region in the emulsion surfaces. The large blue shift in λ_{max} and the highest anisotropy value of 6-AS indicate that the hydrophobicity and the order of the acyl chain are significantly increased around the rigid sterol ring of Chol. These results show that cholesterol enrichment brings about changes in surface properties of emulsions, i.e., PC headgroup separation and acyl chain condensation, which could affect the binding of apolipoproteins or amphipathic helices to emulsion particles.

Peptide Binding to Emulsion Particles. We investigated the effect of Chol on binding of Ac-18A-NH_2 and Ac-18G*-NH_2 by ultracentrifugation assay. Figure 3 shows the binding isotherms of the peptides to TO-PC and TO-PC/Chol emulsions. The binding behavior was described as Langmuir type isotherm, and the dissociation constant (K_d) and the binding maximum (N) were obtained (Table 1). In the presence of Chol, the affinity ($1/K_d$) of Ac-18A-NH_2 was increased, whereas that of Ac-18G*-NH_2 was decreased, although there were no significant changes in the N values of either peptide. The N values of Ac-18A-NH_2 were about twofold larger than those of Ac-18G*-NH_2. These results suggest that the charge distribution of the amphipathic helix plays an important role in binding to emulsions, in response to Chol enrichment of the particle surfaces.

α-Helical Content. To explore the effects of Chol on the secondary structures of the peptides, far-UV CD spectral measurements were performed in the presence of TO-PC or TO-PC/Chol emulsions (Figure 4). Under these conditions, about the same percentage (40%) of the peptide molecules was bound to emulsions as deduced from the binding isotherms. Similar measurements were also performed in the absence of lipids. Ac-18A-NH_2 and Ac-18G*-NH_2 (10 μM) showed similar helical contents in a buffer (21% and 24%, respectively) and increased their helicity upon interaction with emulsions. In TO-PC emulsions, the helical contents of Ac-18A-NH_2 (67%) was much higher than that of Ac-18G*-NH_2 (42%). In the presence of Chol, the helical content of Ac-18A-NH_2 was decreased to 50%, while there were no significant changes in the helicity of Ac-18G*-NH_2 (41%). We also measured their CD spectra in TFE to estimate their α-helical contents in a relatively hydrophobic environment. In TFE, hydrogen bonding of amide protons to the solvent is decreased because of its lower basicity, which strengthens intramolecular hydrogen bonds and thereby stabilizes helical conformation.[35−37] TFE has also been shown to interrupt interhelical hydrophobic interactions because of its low dielectric constant.[38] In this solvent, therefore, the peptides are considered to adopt monomeric-helical structures. The helical contents were estimated to be 66% and 61% for Ac-18A-NH_2 and Ac-18G*-NH_2, respectively. Thus, as well as in a buffer, the two peptides were shown to have similar helical contents in TFE.

Location of the Trp Residue in Emulsion Surface Monolayers. To clarify the location of the Trp residues of the two peptides in emulsion surface monolayers, fluorescence-quenching experiments were carried out. Since there is spectral overlap between Trp emission and *n*-AS absorption, FRET occurs between Trp (donor) and *n*-AS (acceptor). The closer the Trp residues of the peptides are located to the anthroyloxy moieties of *n*-AS in phospholipid monolayers, the more efficiently they transfer energy, and consequently, quenching of Trp fluorescence occurs (i.e., larger values of F_0/F). Since the quencher concentration was kept constant in all samples, the values of F_0/F, which serve as an indicator of the proximity of the quenchers (anthroyloxy moieties of *n*-AS) to the Trp residue, could be compared among different samples. In the absence of Chol, the F_0/F value of Ac-18A-NH_2 was highest in the 6-AS-labeled emulsions (Figure 5A), indicating that the Trp residue of Ac-18A-NH_2 penetrates deeply into the hydrocarbon region. The Trp fluorescence from Ac-18G*-NH_2 was also quenched most efficiently by 6-AS (Figure 5B), but the quenching by 12-AS is significantly less effective than for Ac-18A-NH_2, suggesting the shallower binding to TO-PC emulsions. In the presence of Chol, both peptides represented the largest F_0/F value in 2-AS-labeled emulsions and the value was decreased with an increase in the "*n*"-number (i.e., deeper location of the quencher), suggesting that Chol enrichment on the particle surface leads to shallower location of these peptides.

DISCUSSION

Peptide Location in Emulsions. Mishra et al. previously reported that Ac-18A-NH_2 analogues with shortened hydrocarbon side chains of interfacial lysine residues or with reversed charge distribution compared with Ac-18A-NH_2 showed decreased penetration to lipid bilayers.[14] From their data, it was confirmed that the snorkel effect of interfacial lysine or class A charge distribution is favorable for deeper penetration of Ac-18A-NH_2.

dx.doi.org/10.1021/jp207062h |J. Phys. Chem. B 2012, 116, 476–482

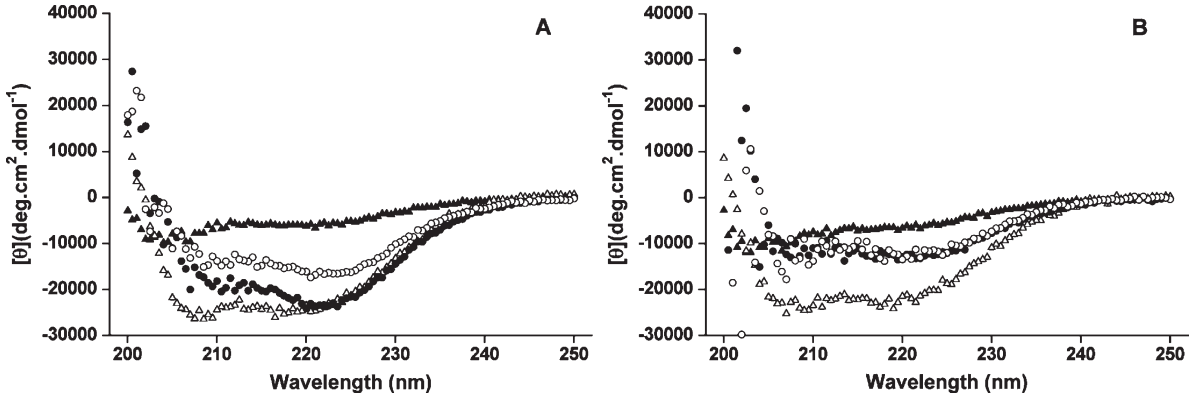

Figure 4. Far-UV CD spectra of Ac-18A-NH_2 (A) and Ac-18G*-NH_2 (B) in a buffer (closed triangles), 50% (v/v) TFE (open triangles), TO-PC emulsions (closed circles), and TO-PC/Chol emulsions (open circles).

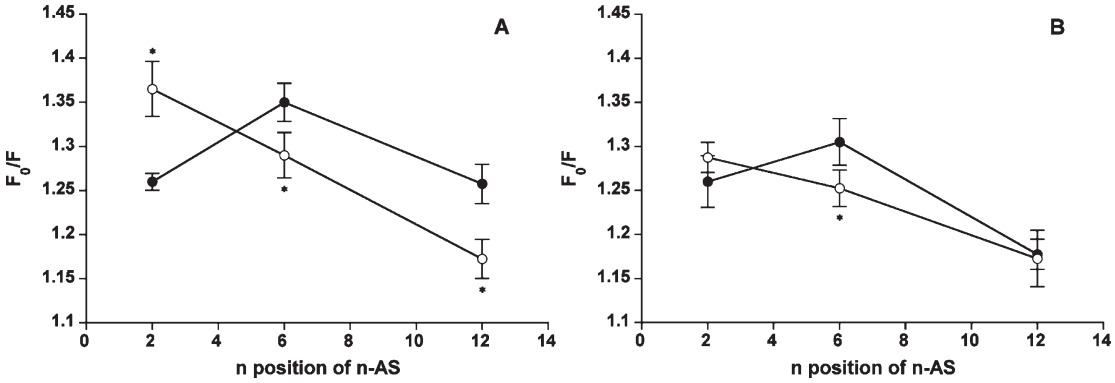

Figure 5. Trp quenching efficiency (F_0/F) of Ac-18A-NH_2 (A) and Ac-18G*-NH_2 (B) bound to TO-PC (closed circles) and TO-PC/Chol (open circles) emulsions by *n*-AS. F_0/F values are plotted against *n*. *$p < 0.05$, significantly different from TO-PC emulsions.

Our quenching data revealed the deeper penetration of Ac-18A-NH_2 into the hydrocarbon region of TO-PC emulsions compared to Ac-18G*-NH_2, which has random charge distribution (Figure 5). This result supports the snorkeling of lysine side chain in emulsion monolayers. We also showed that the location of Ac-18A-NH_2 was more susceptible to Chol than that of Ac-18G*-NH_2. Fluorescence measurements revealed that Chol increased the lipid molecular order and thereby reduced the conformational flexibility of PC acyl chains at any depth in the hydrocarbon region of surface layers (Figure 2). This is in accord with a previous report on the physical states of emulsions.[3] According to the snorkel model, Ac-18A-NH_2 is expected to bind to emulsions with its long hydrocarbon side chains of the interfacial lysine residues deeply inserted into the acyl chain region. The motional restriction induced by Chol is, therefore, unfavorable for the insertion of Ac-18A-NH_2 with the "snorkeling" structure, which leads to a shallower location in the presence of Chol. Judging from the most efficient quenching of Trp fluorescence by 6-AS in TO-PC emulsions and by 2-AS in TO-PC/Chol emulsions (Figure 5A), the Ac-18A-NH_2 Trp residue is thought to be located in the hydrocarbon interior in the absence of Chol and be pushed up toward the membrane interfacial region in the presence of Chol. A similar effect of Chol on the location of Ac-18A-NH_2 in large unilamellar vesicles has been reported previously.[20]

Conformation of the Peptides. By subtraction of the contribution of the free peptides, Ac-18A-NH_2 is assumed to be fully helical in TO-PC emulsions, whereas Ac-18G*-NH_2 adopts a partially helical conformation in either the absence or presence of Chol. Furthermore, although Ac-18A-NH_2 reduced its helicity in the presence of Chol, it still maintained a more helical structure than Ac-18G*-NH_2. Since the amino acid compositions of the two peptides are identical, the helix-forming propensities of individual residues, a contributing factor to helix stability,[39] make no difference in the helix-forming abilities of the whole peptides. It is proposed that intrahelical salt bridges between charged amino acids also contribute to the α-helix stability: Particularly, strong interactions are seen at spacings of charged groups at positions $(i, i+3)$ and $(i, i+4)$.[40,41] Judging from their amino acid sequences, however, such interactions between charged residues of Ac-18A-NH_2 are unlikely to be stronger than those of Ac-18G*-NH_2. In fact, they showed similar helical contents in a buffer or TFE (Figure 4), which suggests that the helix-forming abilities of the two peptides in solution are comparable, despite the difference in their primary amino acid sequences. Taken together, the above data indicate that the higher helix stability of Ac-18A-NH_2 in emulsions is due to the favorable interaction of its class A charge distribution with the phospholipid headgroup, i.e., positive/negative charge clusters of Ac-18A-NH_2 and dipole potential of phospholipid monolayer. Therefore, Ac-18A-NH_2 forms more highly helical and compact conformation and hence represents higher binding capacity than Ac-18G*-NH_2, as described later.

Accompanying the shallower binding, Ac-18A-NH_2 decreased its helical content in the presence of Chol. This is possibly due to

the increased rigidity (Figure 2A) and/or decreased electrostatic interactions between the charged residues and the lipid headgroup. On the other hand, no changes in helical content of Ac-18G*-NH_2 were observed. This is presumably because Ac-18G*-NH_2 adopts relatively shallower binding to emulsions even in the absence of Chol, as suggested by the quenching experiment with *n*-AS.

Peptide Binding to Emulsion Surface Monolayers. Irrespective of the presence of Chol, Ac-18A-NH_2 showed about twofold larger binding capacities than those of Ac-18G*-NH_2 (Figure 3, Table 1). This might reflect the difference in the surface area occupied by the two peptides. As is evident from the CD results, Ac-18G*-NH_2 consistently adopted a less helical structure than Ac-18A-NH_2 on binding to emulsions, in both the absence and presence of Chol. Ac-18G*-NH_2 is thus considered to adopt a more "extended" conformation and thereby occupy a larger surface area of emulsions. Chol does not change the helicity of Ac-18G*-NH_2 and consequently gives no influence on the binding capacity. A slight decrease in N value of Ac-18A-NH_2 by Chol (from 14.4 to 12.0 mmol/mol TO, Table 1) can be explained by the reduction in the helicity of the peptide (Figure 4).

Incorporation of Chol into emulsion particles had inverse effects on the binding affinity ($1/K_d$) of Ac-18A-NH_2 and Ac-18G*-NH_2 (Table 1). Curiously, the CD and the quenching measurements revealed reduced penetration (Figure 5A) and helicity (Figure 4A) of Ac-18A-NH_2 in the presence of Chol, which could have decreased the affinity of the peptide to the emulsions. A possible explanation for the increased affinity of Ac-18A-NH_2 in the presence of Chol is an enhanced dipole−dipole interaction between the positive/negative charge clusters of the peptide and the phospholipid headgroup dipoles. Although it is poorly understood for dipoles in emulsions, Chol has been reported to increase dipole potential of phospholipid vesicles, which is ascribed in part to the dipole moment of Chol itself, increased lipid packing, and, most importantly, a decrease in dielectric constant of the lipid headgroup region.[42] In the present study, fluorescence lifetime and the emission maximum of 2-AS manifested the decreased water penetration into near the ester carbonyl group (Figure 2A and B), which suggests a steep drop of the dielectric constant in the region where the dipole potential is located. It is therefore likely that Chol in emulsions increases the dipole potential and thereby increases the affinity of Ac-18A-NH_2 because of the antiparallel arrangement of dipoles between membrane and peptide. The increased dipole potential would be less effective on Ac-18G*-NH_2 because of its random charge distribution. The decreased affinity of Ac-18G*-NH_2 is considered to be a consequence of the increased lipid packing and the headgroup separation induced by Chol (Figure 2), which allows the peptide to bind more "loosely". Although such an effect may also exist in the case of Ac-18A-NH_2, this unfavorable effect is expected to be negligible due to the greater contribution of the favorable factors.

Physiological Implications. Our results support the view that the surface content of Chol is one of the most important factors regulating the lipid-binding properties of apolipoproteins. However, the lipoprotein particles undergo multiple changes, including alterations in size, surface composition, and core composition, which may affect the binding of apolipoproteins,[3,4,24,43] during the metabolic process. It seems, therefore, that no single factor can account for all the changes in binding properties of exchangeable apolipoproteins.

One phenomenon that is closely related to the present results has been reported: Apolipoprotein E (apoE), a major protein component of chylomicron remnants, plays a crucial role in lipoprotein metabolism through specific interactions with cell membrane receptors.[44,45] ApoE is a two-domain protein that contains a 22 kDa N-terminal domain and a 10 kDa C-terminal domain.[46,47] Experimental evidence indicates that these two domains fold independently and have different functional properties: The N-terminal domain is responsible for low-density lipoprotein receptor binding, and the C-terminal domain binds to lipoprotein with a high affinity.[46,48] Secondary structure predictions indicate that the N- and C-terminal domains are predominantly composed of class G* and class A amphipathic helices, respectively.[12] Sakurai et al. revealed that Chol enrichment on emulsion surfaces increases the binding capacity of apoE and thereby promotes emulsion uptake by macrophages.[7] This observation can be explained by the increased/reduced affinity of the class A/G* helices, respectively. That is, Chol enrichment promotes the binding of apoE C-terminal domain instead of N-terminal domain and induces the conformational change of apoE to the bound state that occupies smaller surface area.[49] Class G* amphipathic helices are found in all of the exchangeable apolipoproteins except apoA-II and C-I.[12] Replacement of the class G* with class A helices could also take place among apolipoproteins in response to Chol enrichment in lipoprotein particles and play important roles in their metabolism.

AUTHOR INFORMATION

Corresponding Author

*Tel. +81-75-753-4565; fax +81-75-753-4601; e-mail mnakano@pharm.kyoto-u.ac.jp.

Present Addresses

[†]Ajinomoto Co. Inc., 1-1 Suzuki-cho, Kawasaki-ku, Kawasaki 210−8681, Japan.

[‡]Faculty of Pharmaceutical Sciences, Suzuka University of Medical Science, 3500-3 Minami Tamagaki-cho, Suzuka, Mie 513−8670, Japan.

ACKNOWLEDGMENT

This study was supported by Grants-in-Aid for Scientific Research from the Japanese Ministry of Education, Culture, Sports, Science and Technology (No. 22018015 and 23107718).

REFERENCES

(1) Li, Q. T.; Tilley, L.; Sawyer, W. H.; Looney, F.; Curtain, C. C. *Biochim. Biophys. Acta* **1990**, *1042*, 42–50.

(2) Massey, J. B.; Pownall, H. J. *Biophys. J.* **1998**, *74*, 869–878.

(3) Saito, H.; Minamida, T.; Arimoto, I.; Handa, T.; Miyajima, K. *J. Biol. Chem.* **1996**, *271*, 15515–15520.

(4) Saito, H.; Okuhira, K.; Tsuchimoto, N.; Vertut-Doi, A.; Matsumoto, C.; Tanimoto, T.; Okada, S.; Handa, T. *Lipids* **2001**, *36*, 27–33.

(5) Yamamoto, M.; Morita, S. Y.; Kumon, M.; Kawabe, M.; Nishitsuji, K.; Saito, H.; Vertut-Doi, A.; Nakano, M.; Handa, T. *Biochim. Biophys. Acta* **2003**, *1632*, 31–39.

(6) Granot, E.; Schwiegelshohn, B.; Tabas, I.; Gorecki, M.; Vogel, T.; Carpentier, Y. A.; Deckelbaum, R. J. *Biochemistry* **1994**, *33*, 15190–15197.

(7) Sakurai, A.; Morita, S. Y.; Wakita, K.; Deharu, Y.; Nakano, M.; Handa, T. *J. Lipid Res.* **2005**, *46*, 2214–2220.

(8) Maranhao, R. C.; Tercyak, A. M.; Redgrave, T. G. *Biochim. Biophys. Acta* **1986**, *875*, 247–255.

(9) Morita, S. Y.; Sakurai, A.; Nakano, M.; Kitagawa, S.; Handa, T. *Lipids* **2011**, *46*, 323–332.

(10) Saito, H.; Miyako, Y.; Handa, T.; Miyajima, K. *J. Lipid Res.* **1997**, *38*, 287–294.
(11) Segrest, J. P.; De Loof, H.; Dohlman, J. G.; Brouillette, C. G.; Anantharamaiah, G. M. *Proteins* **1990**, *8*, 103–117.
(12) Segrest, J. P.; Jones, M. K.; De Loof, H.; Brouillette, C. G.; Venkatachalapathi, Y. V.; Anantharamaiah, G. M. *J. Lipid Res.* **1992**, *33*, 141–166.
(13) Segrest, J. P.; Garber, D. W.; Brouillette, C. G.; Harvey, S. C.; Anantharamaiah, G. M. *Adv. Protein Chem.* **1994**, *45*, 303–369.
(14) Mishra, V. K.; Palgunachari, M. N.; Segrest, J. P.; Anantharamaiah, G. M. *J. Biol. Chem.* **1994**, *269*, 7185–7191.
(15) Mishra, V. K.; Palgunachari, M. N. *Biochemistry* **1996**, *35*, 11210–11220.
(16) Mishra, V. K.; Palgunachari, M. N.; Datta, G.; Phillips, M. C.; Lund-Katz, S.; Adeyeye, S. O.; Segrest, J. P.; Anantharamaiah, G. M. *Biochemistry* **1998**, *37*, 10313–10324.
(17) Polozov, I. V.; Polozova, A. I.; Molotkovsky, J. G.; Epand, R. M. *Biochim. Biophys. Acta* **1997**, *1328*, 125–139.
(18) Clayton, A. H.; Sawyer, W. H. *Biophys. J.* **2000**, *79*, 1066–1073.
(19) Datta, G.; Chaddha, M.; Hama, S.; Navab, M.; Fogelman, A. M.; Garber, D. W.; Mishra, V. K.; Epand, R. M.; Epand, R. F.; Lund-Katz, S.; Phillips, M. C.; Segrest, J. P.; Anantharamaiah, G. M. *J. Lipid Res.* **2001**, *42*, 1096–1104.
(20) Egashira, M.; Gorbenko, G.; Tanaka, M.; Saito, H.; Molotkovsky, J.; Nakano, M.; Handa, T. *Biochemistry* **2002**, *41*, 4165–4172.
(21) Kanellis, P.; Romans, A. Y.; Johnson, B. J.; Kercret, H.; Chiovetti, R., Jr.; Allen, T. M.; Segrest, J. P. *J. Biol. Chem.* **1980**, *255*, 11464–11472.
(22) Anantharamaiah, G. M.; Jones, J. L.; Brouillette, C. G.; Schmidt, C. F.; Chung, B. H.; Hughes, T. A.; Bhown, A. S.; Segrest, J. P. *J. Biol. Chem.* **1985**, *260*, 10248–10255.
(23) Saito, H.; Nishiwaki, K.; Handa, T.; Ito, S.; Miyajima, K. *Langmuir* **1995**, *11*, 3742–3747.
(24) Saito, H.; Tanaka, M.; Okamura, E.; Kimura, T.; Nakahara, M.; Handa, T. *Langmuir* **2001**, *17*, 2528–2532.
(25) Morrisett, J. D.; David, J. S.; Pownall, H. J.; Gotto, A. M., Jr. *Biochemistry* **1973**, *12*, 1290–1299.
(26) Waggoner, A. S.; Stryer, L. *Proc. Natl. Acad. Sci. U.S.A.* **1970**, *67*, 579–589.
(27) Asuncion-Punzalan, E.; Kachel, K.; London, E. *Biochemistry* **1998**, *37*, 4603–4611.
(28) Abrams, F. S.; Chattopadhyay, A.; London, E. *Biochemistry* **1992**, *31*, 5322–5327.
(29) Epand, R. M.; Leon, B. T. *Biochemistry* **1992**, *31*, 1550–1554.
(30) Macanita, A. L.; Costa, F. P.; Costa, S. M. B.; Melo, E. C.; Santos, H. *J. Phys. Chem.* **1989**, *93*, 336–343.
(31) Miyazaki, M.; Nakano, M.; Fukuda, M.; Handa, T. *Biochemistry* **2009**, *48*, 7756–7763.
(32) Nakano, M.; Fukuda, M.; Kudo, T.; Miyazaki, M.; Wada, Y.; Matsuzaki, N.; Endo, H.; Handa, T. *J. Am. Chem. Soc.* **2009**, *131*, 8308–8312.
(33) Fukuda, M.; Nakano, M.; Miyazaki, M.; Handa, T. *J. Phys. Chem. B* **2010**, *114*, 8228–8234.
(34) Miyazaki, M.; Tajima, Y.; Handa, T.; Nakano, M. *J. Phys. Chem. B* **2010**, *114*, 12376–12382.
(35) Nelson, J. W.; Kallenbach, N. R. *Proteins* **1986**, *1*, 211–217.
(36) Sonnichsen, F. D.; Van Eyk, J. E.; Hodges, R. S.; Sykes, B. D. *Biochemistry* **1992**, *31*, 8790–8798.
(37) Zhou, N. E.; Kay, C. M.; Sykes, B. D.; Hodges, R. S. *Biochemistry* **1993**, *32*, 6190–6197.
(38) Lau, S. Y. M.; Taneja, A. K.; Hodges, R. S. *J. Chromatogr.* **1984**, *317*, 129–140.
(39) Chakrabartty, A.; Baldwin, R. L. *Adv. Protein Chem.* **1995**, *46*, 141–176.
(40) Marqusee, S.; Baldwin, R. L. *Proc. Natl. Acad. Sci. U.S.A.* **1987**, *84*, 8898–8902.
(41) Spek, E. J.; Bui, A. H.; Lu, M.; Kallenbach, N. R. *Protein Sci.* **1998**, *7*, 2431–2437.
(42) Starke-Peterkovic, T.; Turner, N.; Vitha, M. F.; Waller, M. P.; Hibbs, D. E.; Clarke, R. J. *Biophys. J.* **2006**, *90*, 4060–4070.
(43) Tanaka, M.; Saito, H.; Dhanasekaran, P.; Wehrli, S.; Handa, T.; Lund-Katz, S.; Phillips, M. C. *Biochemistry* **2005**, *44*, 10689–10695.
(44) Yamamoto, T.; Bujo, H. *Curr. Opin. Lipidol.* **1996**, *7*, 298–302.
(45) Mahley, R. W.; Ji, Z. S. *J. Lipid Res.* **1999**, *40*, 1–16.
(46) Weisgraber, K. H.; Rall, S. C., Jr.; Mahley, R. W. *J. Biol. Chem.* **1981**, *256*, 9077–9083.
(47) Wetterau, J. R.; Aggerbeck, L. P.; Rall, S. C., Jr.; Weisgraber, K. H. *J. Biol. Chem.* **1988**, *263*, 6240–6248.
(48) Aggerbeck, L. P.; Wetterau, J. R.; Weisgraber, K. H.; Wu, C. S.; Lindgren, F. T. *J. Biol. Chem.* **1988**, *263*, 6249–6258.
(49) Narayanaswami, V.; Ryan, R. O. *Biochim. Biophys. Acta* **2000**, *1483*, 15–36.